

EUROPEAN ORGANIZATION FOR NUCLEAR RESEARCH

[Proposal/Letter of Intent/Addendum ...] to the ISOLDE and Neutron Time-of-Flight Committee// **Proposals for ISOLDE low-energy experiments**

Study of Interaction of ^8He with ^{209}Bi sub-barrier energy

May 29 wednesday

[Lukyanov S.M., Astabayan R., Penionzhkevich Yu.E., Revenko R., Skobelev N.]¹,
[Kuterbekov K.A., Kabyshev A.M., Urozaev D.A., Nurmukhanbetova A.K.]²,
[F. de Oliveira, A.Navin]³,
[S. Grévy, J. C. Angélique]⁴,
[A. Buta, C. Borcea, R. Borcea , S. Iulian , F. Negoita,]⁵,

¹ [Joint Institute for Nuclear Research, Dubna, Russia]

²[L.N. Gumilyov Eurasian National University, Astana, Kazakhstan]

³[GANIL, France]

⁴[LPC, Caen, France]

⁵[IFIN-HH, Bucharest-Magurele, Romania]

Spokesperson(s): **Lukyanov S.M.**, (e-mail: lukyan@nrmil.jinr.ru);
Kuterbekov K.A., (e-mail: kkuterbekov@gmail.com)
Contact: *Lukyanov S.M.*, (e-mail: lukyan@nrmil.jinr.ru)

Abstract

Excitation functions for evaporation residues in the reaction $^{209}\text{Bi}(^8\text{He}, xn)^{217-xn}\text{At}$ are proposed for measurement at the ISOLDE facility. A coincidence between neutron and alpha particles allows to get on break-up- fusion and direct breakup phenomena of ^8He .

Study of Interaction of ^8He with ^{209}Bi sub-barrier energy

1. Motivation

It has been found long ago that the fusion of stable nuclei at energies close to the Coulomb barrier strongly depends on the coupling with other reaction channels, in particular with direct reactions [1, 2]. In the case of some light neutron-rich nuclei an extended distribution of nuclear matter is observed and the presence of valence neutrons can lead to the formation of a neutron halo or skin, characterized by small separation energy of the constituent nucleons, $^6, ^8\text{He}$ are such examples. The reactions with halo nuclei have aroused much interest and continue to be a challenge both to experiment and theory. In particular, much effort has been devoted to studying near-barrier fusion of light weakly bound nuclei. What concerns the interaction of the neutron-rich nuclei $^6, ^8\text{He}$ with stable targets, one can expect increased fusion cross-section due to the reduction of the reaction Coulomb barrier because of the larger radius. On the other hand, the weak binding of the halo neutrons leads to a higher breakup probability of the nuclei which, in turn, reduces the fusion cross-section.

If breakup occurs, consequent capture of the residual nucleus (the core) by the target nucleus or transfer of nucleons without any further interaction between the nuclei can take place. The exchange of one or several nucleons between the target and projectile, inelastic scattering, etc. are also probable. However, if the couplings between fusion and transfer reactions with positive Q-values are taken into account, it is expected that the fusion involving ^6He will be enhanced [3,4] similarly to the cases observed for stable beams [1, 2, 5]. In any case, the variety of processes makes it difficult to analyze the



experimental data and requires the consideration of all possible reaction channels. Fusion and breakup reactions with halo nuclei have been studied by different groups. A detailed picture of the situation both from experimental and theoretical point of view can be found in the recently published reviews [6, 7].

In ref. [8] we have presented results on the measurements of the excitation functions for fusion and transfer products in ${}^6\text{He}$ -induced reactions on ${}^{197}\text{Au}$ and ${}^{206}\text{Pb}$ in a wide incident energy range including deep sub-barrier energies. The experiments were performed at the accelerator complex for radioactive beams DRIBs in Dubna, the ${}^6\text{He}$ beam intensity reaching 2×10^7 pps at 10 AMeV. It was found that the transfer of one neutron from ${}^6\text{He}$ to the ${}^{197}\text{Au}$ target nucleus at deep sub-barrier energies ($B - E_{\text{cm}} < 15$ MeV) takes place with relatively high probability. The data on fusion reactions, followed by the evaporation of two neutrons: ${}^{206}\text{Pb}({}^6\text{He}, 2n){}^{210}\text{Po}$ and ${}^{197}\text{Au}({}^6\text{He}, 2n){}^{201}\text{Tl}$, at energies close to the Coulomb barrier differ from predictions within the framework of the statistical model for compound-nucleus decay. The observed enhancement in the ${}^{206}\text{Pb}+{}^6\text{He}$ reaction is consistent with a calculation within the model of "sequential fusion" [9]. However, a drawback of the experiment is the rather large energy spread.

The experimental and calculated yield of the ${}^{210}\text{Po}$ isotope from the ${}^{206}\text{Pb}+{}^6\text{He}$ reaction is compared to results from the ${}^4\text{He}+{}^{208}\text{Pb}$ reaction in Fig. 1 (calculated 1n-, 2n, and 3n-evaporation channels; the experiment and calculations for the 1n-channels practically coincide), see ref. [3,4].

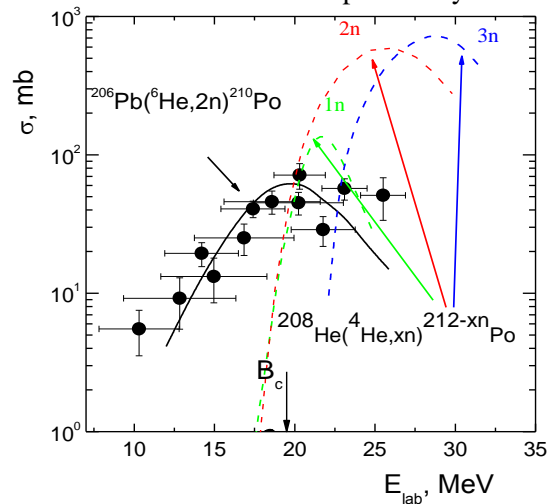
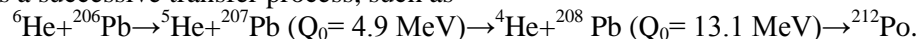


Fig. 1. Excitation functions for the production of evaporation residues in the reactions ${}^6\text{He}+{}^{206}\text{Pb}$ (solid thin curve, calculated using the two-step fusion model for the ${}^6\text{He}+{}^{206}\text{Pb}$ reaction, taking into account the beam energy spread) and ${}^4\text{He}+{}^{208}\text{Pb}$ (dashed curves: green – 1n, red – 2n, and blue – 3n evaporation channels). The symbols (\bullet) are experimental cross-sections for the formation of ${}^{210}\text{Po}$ in the reaction ${}^6\text{He}+{}^{206}\text{Pb}$ [3, 4]. B_c is the Coulomb barrier.

The observed enhancement for the evaporation of two neutrons in the ${}^6\text{He}$ case, as it can be seen from Fig.1 (the thin line), is well described by the mechanism of "sequential fusion" with an intermediate neutron transfer from ${}^6\text{He}$ to the ${}^{206}\text{Pb}$ nucleus with positive Q values. There is a difference in the Q-values of the reactions ${}^4,{}^6\text{He}+{}^{208,}{}^{206}\text{Pb}$, leading to the same $A_{\text{CN}} = {}^{212}\text{Po}$. If we consider the formation of $A_{\text{CN}} = {}^{212}\text{Po}$ as a successive transfer process, such as



The predictions indicate that the high Q-value (13.1 MeV) for neutron transfer may lead to an increase of the effective energy with respect to the barrier (which is about 20 MeV) and hence to an increase of the fusion probability; actually – exactly what is observed in the experiment [3,4].

It should be also noted that in [3,4] unusually large cross section (~ 1 b) was measured at energies below the Coulomb barrier for the production of ${}^{198}\text{Au}$ in the interaction of ${}^6\text{He}$ with a ${}^{197}\text{Au}$ target.

As was already mentioned, it is important to distinguish the different exit reaction channels when a loosely bound nucleus is involved. Several experiments have been performed with this aim. Some of them rely on neutron- α -particle coincidence measurements to study the breakup of ${}^6\text{He}$ on a ${}^{209}\text{Bi}$ target (e.g. [11]). Cross sections for one-neutron and two-neutron transfers have been deduced. However, in our

opinion, a serious disadvantage of such studies is the absence of a direct observation of the residual transfer products $^{210,211}\text{Bi}$.

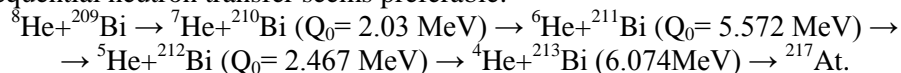
The study of the fusion reaction of ^6He ions with a ^{238}U target was reported in [12] at energies near the fusion barrier. A large fission yield was observed, but according to the authors this enhancement was not related to complete fusion of ^6He with the U-target; it was explained as due to fission following two-neutron transfer to the target [13].

Enhancement in the sub-barrier fusion cross section has been observed in the reaction ^9Li with ^{70}Zn [14], too. A large value of the fusion radius was deduced: $R_B = (12.1 \pm 1.0)$ fm. On the other hand, this result is rather surprising due to the absence of a prominent halo structure in the ^9Li -projectile.

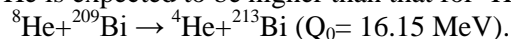
There are a few more experiments, see for example [15,16], aimed to study the fusion and neutron transfer in reactions of ^6He with different targets. However, these measurements have not included all possible exit channels and suffer from low statistics. In any case, the available experimental data is still unable to give a definite qualitative and quantitative identification of all the mechanisms involved in the interaction of weakly-bound nuclei. Obviously, new experimental data will be useful in clarifying this issue.

In this proposal, we focus on the study of the excitation functions for fusion-evaporation and probable breakup-fusion reactions by producing the compound nucleus ^{217}At in two different projectile-target combinations: $^8\text{He} + ^{209}\text{Bi} \rightarrow ^{217}\text{At}^*$ and $^9\text{Li} + ^{208}\text{Pb} \rightarrow ^{217}\text{At}^*$, as it is shown in Fig.2. In principle, the reaction $^9\text{Li} + ^{208}\text{Pb}$ and its comparison to $^8\text{He} + ^{209}\text{Bi}$ could be a subject of a future study, but the case of ^8He is more interesting due to the higher values of Q for the neutron transfer reactions, the higher probability of sequential fusion and the existence of a neutron skin in this projectile.

Similarly to the $^6\text{He} + ^{206}\text{Pb}$ reaction illustrated above, we now consider the case of a ^8He -beam; in this case the sequential neutron transfer seems preferable:



Moreover, the reaction induced by ^8He is of additional interest because the probability of multi-neutron transfer in the case of ^8He is expected to be higher than that for ^6He :



Thus we suggest to irradiate in our experiment heavy targets, such as Bi and Pb. Compared to Zn or Cu [14,15], the Bi and Pb targets have the advantage of allowing the use of α -spectroscopy to detect evaporation residues instead of γ -ray spectroscopy. The α -particle registration method has a few times larger efficiency – about 50%, compared to only a few percents in the case of γ -ray spectroscopy.

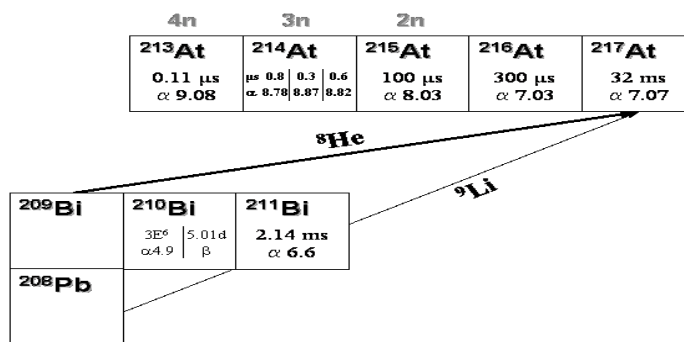


Fig. 2. Diagram of At compound nuclei, produced in different entrance channels.

Fig. 3 presents the calculated excitation functions for the fusion reaction $^8\text{He} + ^{209}\text{Bi} \rightarrow ^{217}\text{At}$, followed by the evaporation of mainly 2-4 neutrons at the energy close to the barrier. Comparison is made between the predictions of the statistical model for decay of a compound nucleus (the code PACE [20] was used) – the dashed lines, marked in the figure by “no neutron transfer”, and of the “sequential fusion” model of ref. [9] – the solid curves (“with neutron transfer”). Accordingly, taking into account the experimental sensitivity, we may expect to get new results for the 3n- and 4n-evaporation channels, and marginally –

for the 2n-channel. In any case, it is expected to observe some enhancement at energies below the Coulomb barrier compared to the calculations with the statistical model.

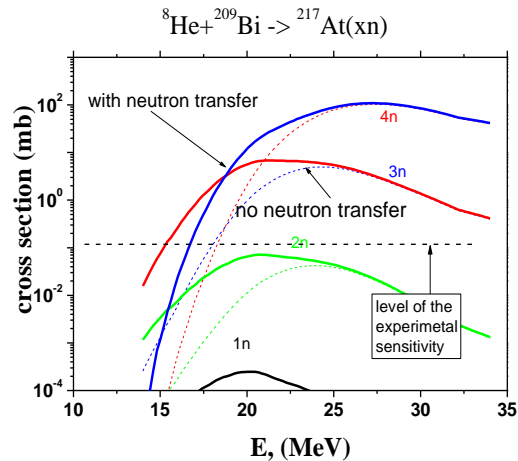


Fig. 3. Calculated excitation functions according to the “sequential fusion” model [9] for the ${}^8\text{He}+{}^{209}\text{Bi}$ reaction leading to the compound nucleus ${}^{217}\text{At}$ compared with expectations according to the statistical model of compound nucleus decay.

Summarizing, our aim is to measure cross sections for the evaporation residues (xn channels), emitted following the fusion of ${}^8\text{He}$ with ${}^{209}\text{Bi}$ for beam energies close to the Coulomb barrier. The experimental results will be compared with calculations within the statistical and the “sequential fusion” models [9,20]. Measuring the xn -transfer channels to Bi-isotopes will allow comparison with the results for the ${}^6\text{He}+{}^{197}\text{Au}$ reaction [3,4].

2. Experimental Set-up:

As can be seen from Fig. 2, experimentally we have to measure short-lived nuclei-residues (mainly ${}^{215-213}\text{At}$) after 2n, 3n and 4n neutron evaporation, respectively. For the short-living residues we shall use on-line measurement with the setup, whose layout is shown schematically in Fig. 4. This setup consists of three parts: a secondary beam monitoring system (including wedge and two plastic scintillators), a system for measuring the xn evaporation residues of the produced compound nuclei, as well as fission fragments, and a third part for the study of breakup of weakly-bound projectiles (the “fragmentation part”).

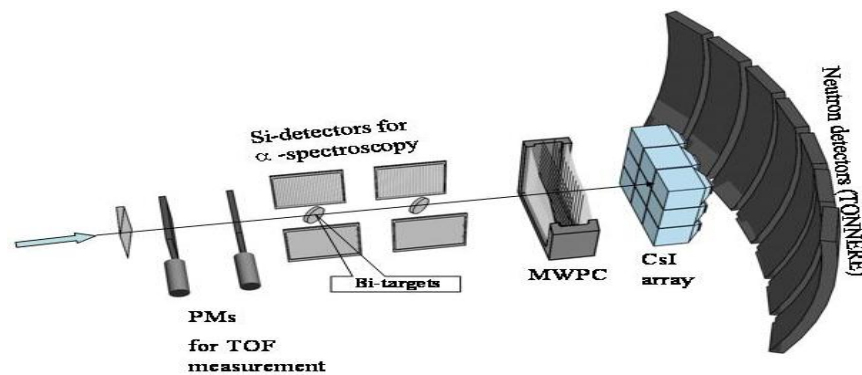


Fig. 4. Layout of the experimental set-up.

The secondary beam monitoring system, as a part of the setup, allows to determine the energy of the beam before impinging on the target by means of event-by-event coincidence measurement of the TOF of the beam particles and the reaction events. The time resolution of the system is less than 1.5 ns corresponding to an energy resolution better than 0.8 MeV.

The main part of the setup [17] for studying xn -reactions induced by the secondary radioactive beams has already been constructed and used in other experiments. It allows simultaneous measurement of α -particle and fission fragment energy spectra. A set of two targets can be used so as to ensure higher

statistics. Two silicon detectors, located at 90° to the secondary beam direction, face each target, thus covering about 50% of the solid angle. Thus excitation functions of fusion-fission reactions can be measured for the studied reaction $^8\text{He}+^{209}\text{Bi}$. By measuring the α -particles, identification of evaporation residues can be done.

As an example, a typical energy spectrum of alpha radioactivity, accumulated in the reaction $^7\text{Li}+^{208}\text{Pb}$ and obtained from an “on-line” measurement is shown in Fig. 5. It can be seen that the identification of the different evaporation channels (3n – corresponding to ^{212}At , and 4n – corresponding to ^{211}At and its daughter ^{211}Po) is highly reliable, the energy resolution of the alpha-spectrometer being about 80 keV.

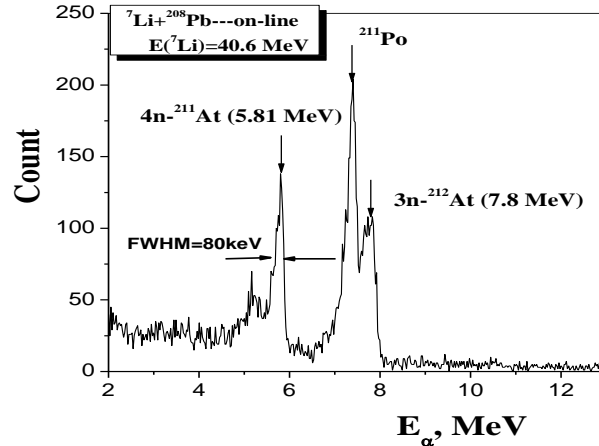


Fig. 5. α -particle energy spectrum for the evaporation residues in the reaction ($^7\text{Li}+^{208}\text{Pb}\rightarrow^{215-xn}\text{At}$) measured “on-line”.

For the study of the breakup of the ^8He projectiles, we plan to use the so called “fragmentation part”: it is a conjunction of Si-CsI telescopes with neutron detectors from the TONNERRE setup [18]. The Si-CsI-array is used for the energy and particle identification of the light fragment emitted at forward direction after breakup. For the precise angle measurement, multi-wire position-sensitive proportional detectors (“MWPC”) will be used in front of the Si-CsI-array.

Different light particles can be produced via two-neutron transfer, one-neutron transfer, direct projectile breakup, etc. For example, detailed analysis of neutron-alpha correlations from the breakup of ^6He on a Bi target has been reported in [11]. The authors claim to have distinguished the three possible mechanisms that could yield the α -particles (two-neutron transfer followed by evaporation, one neutron transfer followed by ^5He breakup and direct projectile breakup) by the distinctive neutron angular distribution (or neutron- α -particle angular correlation) relative to the direction of the emitted charged particles (p, d, t, ^4He and Li).

A similar behaviour should be expected in the case of the neutron-rich ^8He beam, leading to heavy isotopes of Bi, which are shown in Fig. 2. The “fragmentation” part of the setup could give information about the breakup process of the neutron-rich He on Bi. Information about neutron transfer could be extracted from the α -n coincidence, as was performed in Ref. [11]. However, another possibility is to analyze “off-line” by α - and/or γ -measurements the Bi targets: in particular, the cross section for 1n-transfer leading to the isotope ^{210}Bi ($T_{1/2} \approx 5$ d) can be estimated by γ -measurement of its direct decay or by α -measurement of the accumulated radioactivity of ^{210}Po , which will be produced after β -decay of ^{210}Bi . Special electronics tuning might give the possibility to measure other xn-transfers “on-line”.

3. Beam Time Request and Estimated Production Rates:

For the energy and efficiency calibration of the detectors we would like to have 5UTs of ^6He for the reaction $^6\text{He} + \text{Bi}$ target.

We request 7-days to study the reaction induced by ^8He beam with intensity of up to 1.0×10^5 pps on the ^{209}Bi -targets with thickness $700 \mu\text{g}/\text{cm}^2$ each. The expected production rates as a function of the cross section for the xn-channels are shown in the table below:

Events/hour	0.3	3	30
--------------------	-----	---	----

σ (mb)	0.1	1	10
---------------	-----	---	----

Practically, one may reach 1 mb cross section level in this experiment using a secondary beam of ^8He ions. It means that we shall be able to get 3n- and 4n-evaporation residues with reasonable statistics. The beam time request for ^8He is shown in this table:

Time Request	Beam energy	Main goal	Expected events
One-day run	E1 = 25 (MeV)	3n, 4n	600, 1200
Two-days run	E2 = 20 (MeV)	3n, 4n	800, 800
Three-days run	E3 = 15 (MeV)	2n, 3n	~1, 210
Total UTs for ^8He	21UTs		

Totally we need 21UTs to study fusion, break-up and transfer of ^8He ions on ^{209}Bi at three values of the bombarding energies.

Summary of requested shifts:

Our aim is to measure cross sections for the evaporation residues (xn channels), emitted following the fusion of ^8He with ^{209}Bi for beam energies close to the Coulomb barrier. The experimental results will be compared with calculations within the statistical and the “sequential fusion” models [9,20]. Measuring the xn-transfer channels to Bi-isotopes will allow comparison with the results for the $^6\text{He}+^{197}\text{Au}$ reaction [3,4].

References:

1. M. Beckerman. Rep. Prog. Phys. 51 (1988) 1047 and references therein.
2. R.A. Broglia, C.H. Dasso, S. Landowne, A. Winther. Phys. Rev. C 27 (1983) 2433R and references therein.
3. Yu.E. Penionzhkevich, V.I. Zagrebaev, S.M. Lukyanov, R. Kalpakchieva. Phys. Rev. Lett. 96 (2003)162.
4. Yu.E. Penionzhkevich *et al.* Eur. Phys. J. A 31 (2007) 185.
5. S. Saha, Y.K. Agarwal. Nucl. Phys. A 601 (1996) 251.
6. J.F. Liang, C. Signorini. Int. J. Mod. Phys. E 14 (2005) 1121.
7. L.F. Canto, P.R.S. Gomes, R. Donangelo, M.S. Hussein. Phys. Rep. 424 (2006) 1.
8. Yu.E. Penionzhkevich, Nucl. Phys. A 588 (1995) 259c; Yu.E. Penionzhkevich *et al.* Eur. Phys. J. A 13 (2002) 123.
9. V.I. Zagrebaev. Phys. Rev. C 67 (2003) 061601(R); Prog. Theor. Phys. Suppl. 154 (2004) 122.
10. A.R. Barnet and J.S. Lilley. Phys. Rev. C 9 (1974) 2010.
11. J.J. Ko lata *et al.* Phys. Rev. C 75 (2007) 031302(R) and references therein.
12. M. Trotta *et al.*, Phys. Rev. Lett. 84 (2000) 2342.
13. R. Raabe, J. L. Sida, J. L. Charvet *et al.* Nature 431 (2004) 823.
14. W. Loveland, A. M. Vinodkumar, R. S. Naik *et al.* Phys. Rev. C 74 (2006) 064609.
15. A. Navin *et al.* Phys. Rev. C 70 (2004) 044601.
16. A. Di Pietro *et al.*, Phys. Rev. C 69 (2004) 044613.
17. A.A. Hassan, S.M. Lukyanov, R. Kalpakchieva *et al.* Phys. Atomic Nuclei 66 (2003) 1659.
18. A.A. Hassan. Ph.D thesis, FLNR, JINR, Dubna, Russia.
19. A. Buta *et al.* Nucl. Instrum. Methods Phys. Res. A 455 (2002) 412.
20. PACE4 code, <http://www.nscl.msu.edu/lise>

Appendix

DESCRIPTION OF THE PROPOSED EXPERIMENT

The experimental setup comprises: *(name the fixed-ISOLDE installations, as well as flexible elements of the experiment)*

Part of the Choose an item.	Availability	Design and manufacturing
[if relevant, name fixed ISOLDE installation: COLLAPS, CRIS, ISOLTRAP, MINIBALL + only CD, MINIBALL + T-REX, NICOLE, SSP-GLM chamber, SSP-GHM chamber, or WITCH]	<input checked="" type="checkbox"/> Existing	<input checked="" type="checkbox"/> To be used without any modification
[Part 1 of experiment/ equipment]	<input type="checkbox"/> Existing <input type="checkbox"/> New	<input type="checkbox"/> To be used without any modification <input type="checkbox"/> To be modified <input type="checkbox"/> Standard equipment supplied by a manufacturer <input type="checkbox"/> CERN/collaboration responsible for the design and/or manufacturing
[Part 2 experiment/ equipment]	<input type="checkbox"/> Existing <input type="checkbox"/> New	<input type="checkbox"/> To be used without any modification <input type="checkbox"/> To be modified <input type="checkbox"/> Standard equipment supplied by a manufacturer <input type="checkbox"/> CERN/collaboration responsible for the design and/or manufacturing
[insert lines if needed]		

HAZARDS GENERATED BY THE EXPERIMENT

(if using fixed installation) Hazards named in the document relevant for the fixed [COLLAPS, CRIS, ISOLTRAP, MINIBALL + only CD, MINIBALL + T-REX, NICOLE, SSP-GLM chamber, SSP-GHM chamber, or WITCH] installation.

Additional hazards:

Hazards			
	[Part 1 of the experiment/equipment]	[Part 2 of the experiment/equipment]	[Part 3 of the experiment/equipment]
Thermodynamic and fluidic			
Pressure	[pressure][Bar], [volume][l]		
Vacuum			
Temperature	[temperature] [K]		
Heat transfer			
Thermal properties of materials			
Cryogenic fluid	[fluid], [pressure][Bar], [volume][l]		
Electrical and electromagnetic			
Electricity	[voltage] [V], [current][A]		
Static electricity			
Magnetic field	[magnetic field] [T]		
Batteries	<input type="checkbox"/>		
Capacitors	<input type="checkbox"/>		
Ionizing radiation			

Target material	[material]		
Beam particle type (e, p, ions, etc)			
Beam intensity			
Beam energy			
Cooling liquids	[liquid]		
Gases	[gas]		
Calibration sources:	<input type="checkbox"/>		
• Open source	<input type="checkbox"/>		
• Sealed source	<input type="checkbox"/> [ISO standard]		
• Isotope			
• Activity			
Use of activated material:			
• Description	<input type="checkbox"/>		
• Dose rate on contact and in 10 cm distance	[dose][mSV]		
• Isotope			
• Activity			
Non-ionizing radiation			
Laser			
UV light			
Microwaves (300MHz-30 GHz)			
Radiofrequency (1-300MHz)			
Chemical			
Toxic	[chemical agent], [quantity]		
Harmful	[chemical agent], [quantity]		
CMR (carcinogens, mutagens and substances toxic to reproduction)	[chemical agent], [quantity]		
Corrosive	[chemical agent], [quantity]		
Irritant	[chemical agent], [quantity]		
Flammable	[chemical agent], [quantity]		
Oxidizing	[chemical agent], [quantity]		
Explosiveness	[chemical agent], [quantity]		
Asphyxiant	[chemical agent], [quantity]		
Dangerous for the environment	[chemical agent], [quantity]		
Mechanical			
Physical impact or mechanical energy (moving parts)	[location]		
Mechanical properties (Sharp, rough, slippery)	[location]		
Vibration	[location]		
Vehicles and Means of Transport	[location]		
Noise			
Frequency	[frequency],[Hz]		
Intensity			
Physical			
Confined spaces	[location]		
High workplaces	[location]		
Access to high workplaces	[location]		
Obstructions in passageways	[location]		
Manual handling	[location]		
Poor ergonomics	[location]		

0.1 Hazard identification

3.2 Average electrical power requirements (excluding fixed ISOLDE-installation mentioned above):
(make a rough estimate of the total power consumption of the additional equipment used in the experiment) 10kW